Iraqi Journal of Science, 2022, Vol. 63, No. 3, pp: 1265-1276
DOI: 10.24996/ijs.2022.63.3.31

ISSN: 0067-2904

Impact of Varying Viscosity with Hall Current on Peristaltic Flow of Viscoelastic Fluid Through Porous Medium in Irregular Microchannel

Hayat A. Ali
Department of Applied Science, University of Technology, Baghdad, Iraq

Received: 14/6/2021 Accepted: 15/8/2021

Abstract

In this article the peristaltic transport of viscoelastic fluid through irregular microchannel under the effect of Hall current, varying viscosity and porous medium is investigated. The mathematical expressions for the basic flow equations of motion are formulated and transformed into a system of ordinary differential equations by utilizing appropriate non dimensional quantities. The exact solution for the temperature distribution is obtained, while perturbation series solution for the stream function in terms of tiny viscosity parameter is used. Graphical illustrations are presented to capture the physical impact of embedded parameters in the fluid flow i.e. the fluid velocity field, temperature distribution, pressure rise, and trapped bolus. The study shows the opposite effect for Hall current parameter with the magnetic parameter on the flow characteristics.

Keywords: peristaltic flow, varying viscosity, Hall current, porous medium, irregular microchannel.

تأثير اللزوجة المتغيرة مع تيار هول على التدفق التمعجي للسائل اللزج المرن عبر وسط مسامي في قناة متناهية الصغر غير منتظمة

حياة عادل علي

قسم العلوم التطبيقية, الجامعة التكنولوجية, بغداد, العراق

الخلاصة

في هذه المقالة تم توضيح النقل التمعجي للسائل اللزج المرن عبر قناة متناهية الصغر غير المنتظمة تحت تأثير تيار هول ، واللزوجة المتغيرة والوسط المسامي. تمت صياغة التعبيرات الرياضية لمعادلات التدفق الأساسية للحركة وتحويلها إلى نظام من المعادلات التفاضلية العادية عن طريق استخدام الكميات اللابعدية المناسبة .تم الحصول على الحل الدقيق لتوزيع درجة الحرارة بينما تم استخدام سلسلة الاضطراب بالنسبة لمعامل اللزوجة الصغير في ايجاد الحل لدالة التدفق . تم تقديم الرسوم التوضيحية لبيان التأثير المادي للمعلمات المضمنة في تدفق المائع ، أي على سرعة المائع، وتوزيع درجة الحرارة ، وارتفاع الضغط ، والفقاعة المحاصرة. في هذه الدراسة تم توضيح التأثير المعاكس لمعامل تيار هول مع معلمة المغناطيسية على خاصائص التدفق.

1. Introduction

The peristalsis mechanism becomes a great importance in many scientific researches especially in mechanical, and physiological situations as well as in the human body flows in

*Email: Hayat.A.Ali @uotechnology.edu.iq

the esophagus, stomach, and intestines induced a progressive wave of contraction and relaxation trains along the walls of the flexible muscles depending on peristaltic transport. However, in the food process medical devices, and other industries this phenomenon plays a great role in controlling the driven of fluids inside tracts, prevents blockages and keeps apart the fluid contents from the tract boundaries [1,2]. The first progress in peristalsis principle was done by Latham [3], who analyzed the flow of urine through ureter. Then after numerous investigations addressed the peristaltic mechanism under various configurations are cited in [4-6].

The peristaltic transport associates with some tubular organs like small blood vessels, lymphatic vessel, intestine, digestive tract, and bloodstream in tiny conduits, where the viscosity of the fluid shifts over the thickness of the fluid. Assuming the fluid viscosity is a variable (function of space coordinate, and temperature) it helps to understand the complex rheological behaviors of many classical and biological fluids. Therefore, it is extremely useful to include the impact of variable viscosity instead of supposing the viscosity of the fluid to be constant. Ali *et al.* [7] studied the effect of slip condition on the peristaltic transport of MHD viscous fluid in a two-dimensional channel with variable viscosity. An investigation is based on electro-magneto-hydrodynamic flow in micro-channels through slightly corrugated walls impact which is recorded in the existence of variable viscosity by Rashid *et al.* [8]. However, Khan *et al.* [4] employed the regular perturbation method to find the analytic solution for the peristaltic flow of a Jeffrey fluid having variable viscosity through a porous medium in an asymmetric channel. Prakash *et al.* [9] illustrated the effect of variable viscosity on peristaltic transport of a viscoelastic fluid through a tapered microfluidic vessel. Nadeem and Akbar [10] considered variable viscosity effect, and heat transfer on the peristaltic transport of MHD Newtonian fluid.

Hall current have vast impacts for a high magnetic field as in MHD flows. This effect has extensive applications in many aspects which encompasses the devices like power generators, Hall accelerators, refrigeration coils, electric transformers, and spacecraft propulsion. The peristaltic transport in the presence of Hall current has been discussed by various published papers. Krishna *et al.* [11] illustrated the impact of Hall on MHD peristaltic flow of non-Newtonian Jeffery fluid in porous medium in a vertical channel. In 2019 Nabil *et al.* [12] investigated two effect of Hall Currents and Ion Slip on a Peristaltic MHD Nanofluid with Suspended Particles. Asha and Deepa [13] discussed the influence of Hall current, and heat transfer on peristaltic blood flow of a MHD Jeffrey fluid in a vertical asymmetric porous channel.

Keeping in observation the overhead medical, industrial and physiological practical application for Hall current and variable viscosity, our aim in this study is to extend the work of Prakash *et al.* [9] by investigating the effect of Hall current together with porous medium on. The illustration is extended by involving the energy equation, and it is formulated under the effect of magnetic field. As well as the concentration equations is studied. The exact solution for the temperature and concentration fields are found by integration whereas. Perturbation technique series is adopted to obtain the closed form solution for the stream function. Finally, the physically impact of various pertinent parameters on the flow quantities is analyzed graphically.

2. Problem Mathematical Formulation

Consider an incompressible a viscoelastic fluid has a variable viscosity generated by an oscillatory wave travels along the $\check{X}-$axis at fixed speed c through a porous media in a two-dimensional asymmetric non-uniform irregular microchannel. Furthermore the fluid is subjected into a strong magnetic field $B = (0,0,B_0)$. The mathematical description for the physical configuration of the problem in Figure 1 is written as [9]:

$$\check{Y} = H_1(\check{X}, t) = -d_1 - \gamma'\check{X} - \alpha_1 Sin^2\left(\frac{2\pi(\check{X}-ct)}{\lambda}\right) \quad (1)$$

$$\check{Y} = H_2(\check{X}, t) = d_2 + \gamma'\check{X} + \alpha_2 Sin^2\,(2\pi(\check{X}-ct)/\lambda + \emptyset) \quad (2)$$

which $H_1, and\ H_2$ refer to the upper, and lower walls, respectively. α_1, α_2 are the upper, and lower wave amplitudes, t is the time, $(d_1 + d_2)$ is the thickness of the channel, $(\gamma' \ll 1)$is the non-uniform parameter , λ wavelength, and $(\check{X}, \check{Y})are$ the Cartesian coordinates in fixed frame. $\emptyset$ is the phase different and $\emptyset \in [0, \pi]$ such that asymmetric channel with waves out of phase which is expected when $(\emptyset = 0)$, while $(\emptyset = \pi)$ consider waves in phase. Moreover $\alpha_1, \alpha_2, d_1, d_2\ and\ \emptyset$ satisfy the condition.

$$a_1{}^2 + a_2{}^2 + a_1 a_2 d_1 d_2\ cos\emptyset \le (d_1 + d_2)^2 \quad (3)$$

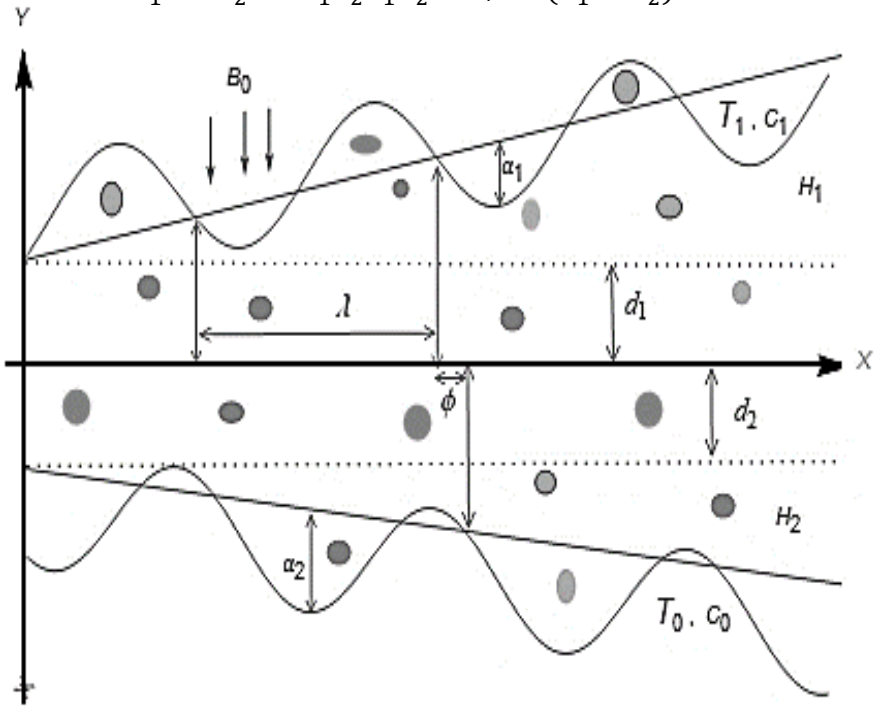

Figure 1-Geometry of the microchannel

The generalized Ohms law contains Hall effects are deduced as [14]:

$$\vec{F} = \vec{J} \times \vec{B}, \quad (4)$$

$$\vec{J} = \sigma[\vec{V} \times \vec{B} - \frac{1}{en}\left(\vec{J} \times \vec{B}\right)], \quad (5)$$

Hence, the magnetic force field is

$$\vec{F} = \left(\frac{-\sigma {B_0}^2 (U - mV)}{1+m^2}, \frac{\sigma {B_0}^2 (V + mU)}{1+m^2}, 0\right) \quad (6)$$

In which $\vec{J}$ is current density, $\vec{V} = (U, V, 0)$ is velocity field, σ represents the electric conductivity of the fluid, B_0 is strength of magnetic field, $n\ is$ the number density of electron, e refers to the electric charge, and $\left(m = \frac{\sigma B_0}{en}\right)$ is the Hall parameter.

The dimensional essentially flow governing equations are represented by continuity, motion in $\check{X}$ and $\check{Y}$ direction, energy, and concentration, they are mathematically constructed respectively as below

$$\frac{\partial U}{\partial \check{X}} + \frac{\partial V}{\partial \check{Y}} = 0 \quad (7)$$

$$\rho\left(\frac{\partial U}{\partial t} + U\frac{\partial U}{\partial \check{X}} + V\frac{\partial U}{\partial \check{Y}}\right) = -\frac{\partial \bar{P}}{\partial \check{X}} + 2\frac{\partial}{\partial \check{X}}\left(\check{\mu}(\check{Y})\frac{\partial U}{\partial \check{X}}\right) + \frac{\partial}{\partial \check{Y}}\left(\check{\mu}(\check{Y})\left(\frac{\partial V}{\partial \check{X}} + \frac{\partial U}{\partial \check{Y}}\right)\right) - \frac{\sigma B_0 (U - mV)}{1+m^2} - \frac{\check{\mu}(\check{Y})}{\kappa_0} U, \quad (8)$$

$$\rho\left(\frac{\partial V}{\partial t}+U\ \frac{\partial V}{\partial \check{X}}+V\ \frac{\partial V}{\partial \check{Y}}\right)=-\frac{\partial \bar{P}}{\partial \check{Y}}+2\frac{\partial}{\partial \check{Y}}\left(\check{\mu}(\check{Y})\frac{\partial V}{\partial \check{Y}}\right)+\frac{\partial}{\partial \check{X}}\left(\check{\mu}(\check{Y})\left(\frac{\partial V}{\partial \check{X}}+\frac{\partial U}{\partial \check{Y}}\right)\right)-\frac{\sigma B_0(V+mU)}{1+m^2}-\frac{\check{\mu}(\check{Y})}{\kappa_0}V, \quad (9)$$

$$\rho c_P\left(\frac{\partial \check{T}}{\partial t}+U\frac{\partial \check{T}}{\partial \check{X}}+V\frac{\partial \check{T}}{\partial \check{Y}}\right)=K\left(\frac{\partial^2 \check{T}}{\partial \check{X}^2}+\frac{\partial^2 \check{T}}{\partial \check{Y}^2}\right)+\frac{D_B K_T}{c_s}\left(\frac{\partial^2 \check{C}}{\partial \check{X}^2}+\frac{\partial^2 \check{C}}{\partial \check{Y}^2}\right)+\frac{\sigma B_0\left(V^2+U^2\right)}{1+m^2}\ , \quad (10)$$

$$\left(\frac{\partial \check{C}}{\partial t}+U\frac{\partial \check{C}}{\partial \check{X}}+V\frac{\partial \check{C}}{\partial \check{Y}}\right)=D_B\left(\frac{\partial^2 \check{C}}{\partial \check{X}^2}+\frac{\partial^2 \check{C}}{\partial \check{Y}^2}\right)+\frac{D_B K_T}{T_m}\left(\frac{\partial^2 \check{T}}{\partial \check{X}^2}+\frac{\partial^2 \check{T}}{\partial \check{Y}^2}\right), \quad (11)$$

Such that σ is the electrical conductivity, K is thermal conductivity, $\kappa_0\ is$ posity parameter, ρ is density, $c_P$is specific heat, $\check{T}$ is the fluid temperature vector, $\bar{P}$ is the pressure, $\check{C}$ is the concentration vector, $D_B$is the Brownian diffusion coefficient, K_T is the thermal diffusion, T_m is the fluid mean temperature, and c_s is the concentration susceptibility.

The associative dimensional slip boundary conditions are [15]

$$\begin{aligned} &U+{\beta_1}^*\frac{\partial U}{\partial \check{Y}}=0\ ,\ \check{T}=T_1\ ,\quad \check{C}=C_1\ \ on\quad \check{Y}=H_1\left(\check{X},t\right),\\ &U-{\beta_1}^*\frac{\partial U}{\partial \check{Y}}=0\quad ,\ \check{T}=T_0\ ,\quad \check{C}=C_0\ \ on\ \check{Y}=H_2\left(\check{X},t\right), \end{aligned} \quad (12)$$

The following dimensionless variables and quantities are given as

$$x=\frac{\check{X}}{\lambda}\ ,y=\frac{\check{Y}}{d_1}\ ,\ u=\frac{U}{c}\ ,v=\frac{V}{c}\ ,h_1=\frac{H_1}{d_1},h_2=\frac{H_2}{d_1}\ ,p=\frac{{d_1}^2\bar{p}}{\lambda\mu c},\delta=\frac{d_1}{\lambda}\ ,u=\frac{\partial\psi}{\partial y}\ ,v=-\delta\frac{\partial\psi}{\partial x},Re=\frac{\rho c d_1}{\mu_0},\ \theta=\frac{\check{T}-T_0}{(T_1-T_0)},Pr=\frac{\mu_0 c_P}{K}\ ,H=\beta_0 d_1\sqrt{\frac{\sigma}{\mu_0}}\ ,E_c=\frac{c^2}{c_P(T_1-T_0)}\ ,Br=E_cPr\ ,\gamma=\frac{\acute{\gamma}}{d_1}\ ,Du=\frac{D_B K_T(C_1-C_0)}{c_P c_s(T_1-T_0)}\ ,a=\frac{\alpha_1}{d_1}\ ,b=\frac{\alpha_2}{d_1}\ ,d=\frac{d_2}{d_1},\kappa=\frac{\kappa_0}{{d_1}^2},\eta=\frac{\check{C}-C_0}{(C_1-C_0)},Sr=\frac{D_B K_T(T_1-T_0)}{\mu_0 T_m(C_1-C_0)},Sc=\frac{\mu_0}{D_B},\mu(y)=\frac{\check{\mu}(\check{Y})}{\mu_0},\beta_1=\frac{{\beta_1}^*}{d_1},u=\frac{\partial\psi}{\partial y},v=-\frac{\partial\psi}{\partial x}, \quad (13)$$

Where $\beta_1$is the slip parameter.

Equations. (7) - (12) will be transformed into the following dimensionless forms

$$\delta\ \frac{\partial u}{\partial x}+\delta\frac{\partial v}{\partial y}=0, \quad (14)$$

$$Re\ \delta\left(\frac{\partial u}{\partial t}+u\ \frac{\partial u}{\partial x}+v\ \frac{\partial u}{\partial y}\right)=-\frac{\partial p}{\partial x}+2\delta^2\left(\mu(y)\frac{\partial^2 u}{\partial x^2}\right)+\delta^2\frac{\partial}{\partial y}\left(\mu(y)\frac{\partial v}{\partial x}\right)+\frac{\partial}{\partial y}\left(\mu(y)\frac{\partial u}{\partial y}\right)-\frac{H^2(u-mv\delta)}{1+m^2}-\frac{\mu(y)}{\kappa}u, \quad (15)$$

$$Re\ \delta^3\left(\frac{\partial v}{\partial t}+u\ \frac{\partial v}{\partial x}+v\ \frac{\partial v}{\partial y}\right)=-\frac{\partial p}{\partial y}+2\delta\frac{\partial}{\partial y}\left(\mu(y)\frac{\partial v}{\partial y}\right)+\delta^2\left(\mu(y)\left(\delta^2\frac{\partial^2 v}{\partial x^2}+\frac{\partial^2 u}{\partial y\partial x}\right)\right)-\frac{\delta H^2(\delta v+mu)}{1+m^2}-\frac{\mu(y)}{\kappa}v \quad (16)$$

$$Re\ \delta\ Pr\left(\frac{\partial\theta}{\partial t}+u\frac{\partial\theta}{\partial x}+v\frac{\partial\theta}{\partial y}\right)=\delta^2\frac{\partial^2\theta}{\partial x^2}+\frac{\partial^2\theta}{\partial y^2}+\delta^2 PrDu\frac{\partial^2\eta}{\partial x^2}+Pr\ Du\frac{\partial^2\eta}{\partial y^2}+\frac{Br\ H^2\left(\delta^2v^2+u^2\right)}{1+m^2}\ , \quad (17)$$

$$ReSc\ \delta\left(\frac{\partial\eta}{\partial t}+u\frac{\partial\eta}{\partial x}+v\frac{\partial\eta}{\partial y}\right)=\frac{1}{Sc}\frac{\partial^2\eta}{\partial y^2}+Sr\left(\delta^2\frac{\partial^2\theta}{\partial x^2}+\frac{\partial^2\theta}{\partial y^2}\right), \quad (18)$$

Adopt the assumptions of long-wavelength approximation and small Reynold's number i.e. dropping terms of order δ and higher equations. (15) -(18) are simplified to

$$\frac{\partial p}{\partial x}=\frac{\partial}{\partial y}\left(\mu(y)\frac{\partial u}{\partial y}\right)-\frac{H^2u}{1+m^2}-\frac{\mu(y)}{\kappa}u, \quad (19)$$

$$\frac{\partial p}{\partial y}=0, \quad (20)$$

$$\frac{\partial^2\theta}{\partial y^2}+Pr\ Du\frac{\partial^2\eta}{\partial y^2}+\frac{Br\ H^2u^2}{1+m^2}=0, \quad (21)$$

$$\frac{1}{Sc}\frac{\partial^2\eta}{\partial y^2}+Sr\frac{\partial^2\theta}{\partial y^2}=0, \quad (22)$$

Associate with the corresponding non-dimensional slip boundary conditions [15].

$$\begin{aligned} &u+\beta_1\frac{\partial u}{\partial y}=0\,,\ \theta=1\,,\quad \eta=1\ on\quad y=h_1(x,t)=-1-\gamma x-a\,Sin^2\left(2\pi(x-t)\right),\\ &u-\beta_1\frac{\partial u}{\partial y}=0\quad,\ \theta=0\,,\quad \eta=0\ on\ y=h_2(x,t)=d+\gamma x+bSin^2\,(2\pi(x-t)\ +\emptyset), \end{aligned} \tag{23}$$

By defining the non-dimensional varying viscosity which is given as below [4]:

$$\mu(y)=1-\beta y, \tag{24}$$

where β is the viscosity coefficient. The time-averaged flux is scripted as

$$Q=\int_{h_1}^{h_2}u(x\,,y,t)dy, \tag{25}$$

So that the dimensionless relationship between F the non-dimensional wave mean flow and Q is derived as

$$F=Q-d-1-2\gamma x, \tag{26}$$

while the pressure rise across unite wavelength is given by

$$\Delta p_\lambda=\int_0^1\frac{dp}{dx}dx, \tag{27}$$

We differentiate the equation (19) with respect to y, and we use the equations (20) and (24), then an equation in terms of stream function $\psi(x,y,t)$ is obtained as bellows:

$$(1-\beta y)\psi_{yyyy}-2\beta\psi_{yyy}-\left(\frac{H^2}{1+m^2}+\frac{(1-\beta y)}{\kappa}\right)\psi_{yy}+\frac{\beta}{\kappa}\psi_y=0, \tag{28}$$

Because of the nonlinearity of equation(28), the exact solution is difficult to be found. Therefore, the perturbation technique will embrace to expand the stream function to small value of viscosity coefficient as [16]

$$\psi=\psi_0+\beta\,\psi_1+O(\beta)^2\,, \tag{29}$$

We substitute equation (29) into equation (23) and equation (28). This leads to the following systems

2.1 Zeroth order system

$$\psi_{0yyyy}-\left(\frac{H^2}{1+m^2}+\frac{1}{\kappa}\right)\psi_{0yy}=0, \tag{30}$$

$$\begin{aligned} &\psi_{0y}+\beta_1\psi_{0yy}=0\,,\ on\quad y=h_1(x,t)=-1-\gamma x-a\,Sin^2\left(2\pi(x-t)\right),\\ &\psi_{0y}-\beta_1\psi_{0yy}=0\quad,\quad on\ y=h_2(x,t)=d+\gamma x+bSin^2\,(2\pi(x-t)\ +\emptyset), \end{aligned} \tag{31}$$

2.2 First order system

$$\psi_{1yyyy}-\left(\frac{H^2}{1+m^2}+\frac{1}{\kappa}\right)\psi_{1yy}-y\psi_{0yyyy}-2\psi_{0yyy}+\frac{y}{\kappa}\psi_{0yy}+\frac{1}{\kappa}\psi_{0y}=0, \tag{32}$$

$$\begin{aligned} &\psi_{1y}+\beta_1\psi_{1yy}=0\,,\ at\quad y=h_1(x,t)=-1-\gamma x-a\,Sin^2\left(2\pi(x-t)\right),\\ &\psi_{1y}-\beta_1\psi_{1yy}=0\quad,\quad at\ y=h_2(x,t)=d+\gamma x+bSin^2\,(2\pi(x-t)\ +\emptyset), \end{aligned} \tag{33}$$

By solving the previous two systems with using of Mathematica 11.3 . The final expression for stream function is given by

$$\psi=\frac{e^{-\epsilon y}(e^{2\epsilon y}c_1+c_2)}{\epsilon^2}+c_3+yc_4+\beta\left(\mathrm{c}_7+y\mathrm{c}_8+\frac{e^{-y\epsilon}\left(L_1c_1e^{2y\epsilon}+c_2L_2+L_34\epsilon^3\right)}{8\epsilon^5\kappa}\right), \tag{34}$$

Where

$\epsilon=(\frac{H^2\kappa+(1+m^2)}{(1+m^2)*\kappa})^{0.5}$, $L_1=(-7-3\epsilon^2\kappa+2y^2\epsilon^2(-1+\epsilon^2\kappa)+y(6\epsilon-2\epsilon^3\kappa))$,

$L_2=(7+3\epsilon^2\kappa+y(6\epsilon-2\epsilon^3\kappa)+y^2(2\epsilon^2-2\epsilon^4\kappa))$, $L_3=(\mathrm{c}_4e^{y\epsilon}y^2+2\kappa(e^{2y\epsilon}\mathrm{c}_5+\mathrm{c}_6))$,

Furthermore, the exact solution for temperature and concentration field is achieved by making benefit of the stream function as follows

$$\theta=$$

$$-\frac{1}{3840(1+m^2)\epsilon^{10}\kappa^2\xi}\mathrm{Br}e^{-2y\epsilon}H^2(15c2^2(64\epsilon^6\kappa^2-32\beta\epsilon^3\kappa L_4+\beta^2L_5)+$$

$$4\mathrm{c}2\epsilon\left(240c4e^{y\epsilon}L_6+\epsilon\left(c1e^{2y\epsilon}y^2\left(-960\epsilon^6\kappa^2-160y\beta\epsilon^4\kappa(1+\epsilon^2\kappa)+\beta^2(20y^2\epsilon^4\kappa(1-\right.\right.\right.$$

$3\epsilon^2\kappa) + 4y^4\epsilon^4(-1+\epsilon^2\kappa)^2 + 15(1+5\epsilon^2\kappa)^2)\big) - 40\beta\epsilon\kappa\Big(3c6\Big(-4\epsilon^3\kappa + \beta\big(-3-2\epsilon^2\kappa + y\epsilon(-3+\epsilon^2\kappa) + y^2\epsilon^2(-1+\epsilon^2\kappa)\big)\Big) + e^{y\epsilon}\epsilon\Big(-6c8\Big(-8\epsilon^3\kappa + \beta\big(-17+3\epsilon^2\kappa + 2y^2\epsilon^2(-1+\epsilon^2\kappa) + 2y\epsilon(-5+3\epsilon^2\kappa)\big)\Big) - c5e^{y\epsilon}y^2\epsilon(-24\epsilon^3\kappa+\beta)\Big)\Big)\Big)\Big) + r1 + y\,r2,$

$L_4 = (-3-2\epsilon^2\kappa + y\epsilon(-3+\epsilon^2\kappa) + y^2\epsilon^2(-1+\epsilon^2\kappa)),$
$L_5 = (71+10\epsilon^2\kappa + 27\epsilon^4\kappa^2 + 4y^4\epsilon^4(-1+\epsilon^2\kappa)^2 - 8y\epsilon(-13+3\epsilon^2\kappa) + 8y^3\epsilon^3(3-4\epsilon^2\kappa+\epsilon^4\kappa^2) - 4y^2\epsilon^2(-17+12\epsilon^2\kappa+\epsilon^4\kappa^2)),$
$L_6 = (-8\epsilon^6\kappa^2 + \beta\epsilon^3\kappa(-33+3\epsilon^2\kappa+6y\epsilon(-3+\epsilon^2\kappa) + 2y^2\epsilon^2(-1+\epsilon^2\kappa)) + \beta^2(-62+26\epsilon^2\kappa + 2y^3\epsilon^3(-1+\epsilon^2\kappa) + 2y^2\epsilon^2(-7+5\epsilon^2\kappa) + y\epsilon(-45+23\epsilon^2\kappa))),$
and
$\eta = \frac{1}{3840(1+m^2)\epsilon^{10}\kappa^2\xi} Bre^{-2y\epsilon}H^2ScSr(15c2^2\Big(64\epsilon^6\kappa^2 - 32\beta\epsilon^3\kappa\big(-3-2\epsilon^2\kappa + y\epsilon(-3+\epsilon^2\kappa) + y^2\epsilon^2(-1+\epsilon^2\kappa)\big) + \beta^2\big(71+10\epsilon^2\kappa+27\epsilon^4\kappa^2 + 4y^4\epsilon^4(-1+\epsilon^2\kappa)^2 - 8y\epsilon(-13+3\epsilon^2\kappa) + 8y^3\epsilon^3(3-4\epsilon^2\kappa+\epsilon^4\kappa^2) - 4y^2\epsilon^2(-17+12\epsilon^2\kappa+\epsilon^4\kappa^2)\big)\Big) + 4c2\epsilon\Big(240c4e^{y\epsilon}\Big(-8\epsilon^6\kappa^2 + \beta\epsilon^3\kappa\big(-33+3\epsilon^2\kappa+6y\epsilon(-3+\epsilon^2\kappa) + 2y^2\epsilon^2(-1+\epsilon^2\kappa)\big) + \beta^2\big(-62+26\epsilon^2\kappa+2y^3\epsilon^3(-1+\epsilon^2\kappa) + 2y^2\epsilon^2(-7+5\epsilon^2\kappa) + y\epsilon(-45+23\epsilon^2\kappa)\big)\Big) + 15(1+5\epsilon^2\kappa)^2\Big) + c6y^2\epsilon(-24\epsilon^3\kappa + \beta(3+15\epsilon^2\kappa - 2y(\epsilon+\epsilon^3\kappa) + y^2(\epsilon^2-\epsilon^4\kappa)))) + r3 + y\,r4$.

The coefficients $c1, c2, c3, c4, c5, c6, c7, c8, r1, r2, r3, r4$ will be obtained by satisfying the given boundary conditions

3. Graphical results and discussions

This part of the paper focuses on the graphical results and analysis the physical effect to emerge important parameters on the flow characteristics that conclude the velocity profile, temperature distribution, heat transfer along the lower wall, and trapping phenomenon for the Newtonian fluid.

Figures 2 and 3 illustrate the impact of Hartman number H, Hall number m ,porosity parameter κ, dimensionless viscosity coefficient β , slip parameter β_1, non-uniform parameter γ, flow rate parameter Q, and phase difference parameter $\emptyset$ on the velocity distribution profile. The parameters, and variables are $a = 0.4, b = 0.03, d = 0.8, x = 0.1, t = 0.1,\ and\ \gamma = 0.1$. It is noticed from the Figures that the velocity profiles attain concave down behavior. In addition the velocity is not symmetric i.e. the result in the central part opposite the response near the walls. Figures 2(a), 2(b) and 2(c) exhibit the influence of H, m and κ on $u(y)$ respectively. It is considered that enhancement of H diminishes the motion of the fluid and henceforth the velocity profile decreases along the whole region, while the velocity arises in the regions $(-1.5 \le y \le -1.1) \cup (0.5 \le y \le 0.9)$. Whereas the increment impact for m and κ on velocity profile are scrutinized along the length of the channel, however the decreasing effect are noticed at some regions near the central part of the channel. The mixed influence of β on $u(y)$ is prescribed through Figure 3(a). While the velocity profile shows two opposite behavior for higher values of $\beta_1$see Figure 3(b). Furthermore, an increasing function of γ on $u(y)$ is portrayed and this is obvious since it causes increase in channel's diameter via Figure 3(c).

Elevation of temperature distribution $\theta(y)$via variation of involved parameters is captured in this subsection through Figures 4 and 5. The discussion is done for the fixed magnitudes $\{a = 0.1, b = 0.9, d = 0.9, Q = 2, \phi = \frac{\pi}{6}, x = 0.2, t = 0.1, \gamma = 1.8\}$. It is

deduced from these plots that the fluid's temperature witnessed variation near the boundaries, while it remains stable in the central part of the channel. The temperature distribution development in response to ascending values of Hartman number H is illustrated in Figure 4(a). Larger values of H reversely effect on $\theta(y)$ due to the fact that the existence of the magnetic field produces a resistance force which declines the fluid's temperature. Similar outcome of $\theta(y)$is recorded upon enhance the porosity parameter κ , Soret number , Dufour number Du and Hall number m via Figures 4(b) ,4(c),5(a), and 5(b) respectively. While Figure 5(c) reveals that the temperature distribution decelerates when the value of Brinkman number Br enhances.

The variation of fluid concentration $\eta(y)$ versus the axial coordinate y with ascending values of Hartman number H, Hall number m ,porosity parameter κ, dimensionless viscosity coefficient β, Prandtl number Pr, Brinkman number Br, and for fixed quantities $a = 0.1, b = 0.9, d = 0.9, Q = 2, \phi = \frac{\pi}{6}, x = 0.2, \beta_1 = 0.3, t = 0.1, \gamma = 1.8, Sc = 1.5, Sr = 0.1$. This is visualized in Figures 6 and 7. The patterns of concentration profile show that the fluid particles are more concentrated near the boundaries of channel whereas it is settle down in the central region. Figure 6(a) highlights the diminishing impact of H on (y) . However, $\eta(y)$ exhibits an increment behavior due to elevate of m, and κ values via Figures 6(b), and 6(c) respectively. Two opposite influence for β on $\eta(y)$ profile is interpreted in Figure 7(a) i.e. the profile increases for$-5 \leq y \leq -3.5$, and decreases for $3.5 \leq y \leq 5$. It is observed from Figures 7(b) and 7(c) that the concentration profile reduces for higher magnitudes of Pr, and Br.

This subsection focuses on the development in pressure rise Δp_λ which is integrated numerically using Mathematica 11.3 against the flow rate Q effected through the following interesting parameters Hartman number H, dimensionless viscosity coefficient β, Hall number m , permeability parameter κ, slip parameter β_1 , and non-uniform parameter γ. This is done for fixed quantities $a = 0.1, b = 0.3, d = 0.2, \phi = \frac{\pi}{6}, y = 0.1, t = 0.1$ via Figures 8 and 9. It is demonstrated that the flow region split into three segments as follows: peristaltic region for $\Delta p_\lambda > 0, and\ Q > 0$, the retrograde pumping region $\Delta p_\lambda > 0, and\ Q < 0$, and the augmented pumping ($\Delta p_\lambda < 0, Q > 0$), while the free pumping is achieved when $\Delta p_\lambda = 0$. Figure 8(a), and 8(b) record the decreasing impact for H and β on the all flow pumping region. Whilst directly effect for m, β_1 and κ on the previous three pumping region that compared with H see Figures 8(c),9(a) and 9(b). It is noticed from Figure 9(c) that for ascending value of γ all the pumping regions increase up to a critical value $Q = 0.7$. However, the pumping diminishes after this value.

The living body fluid flux characteristics like motion of thrombus in blood vessels, and the chyme movement through the gastrointestinal tract are application of an interesting phenomenon in the peristaltic flow which is called trapping. In this phenomenon, an internally circulating fluid bolus formulates by closed streamlines and moves along with the wave. This subsection is allocated to propose the development in the trapping phenomenon versus different values of pertinent parameters. Figures 10, and 11 demonstrate the behavior of Hartman number H and Hall number m on the trapped bolus, respectively. It is evident that H shows a declining impact on trapped bolus meanwhile and this result is obvious since the effect of magnetic forced is represented by Hartman number opposite the fluid flow , the volume, and number of bolus enhances for larger values of m. The opposite effect of the Hall parameter on the Hartmann parameter comes because the first is added to reduce the effect of the magnetic field on the flow and thus increases the velocity of the flow. Qualitatively increasing is response of trapped bolus in size and numbers especially in the upper part of channel against enhancement of permeability parameter , and dimensionless viscosity coefficient β . These are recorded via Figures 12, and 13. However, from Figure 14 we have

visualized that the bolus of fluid have gone down in size via enlarges of time flow rate parameter Q. Figure 15 portrayed rises up in number and magnitude of the trapped bolus for ascending values of slip parameter β_1.

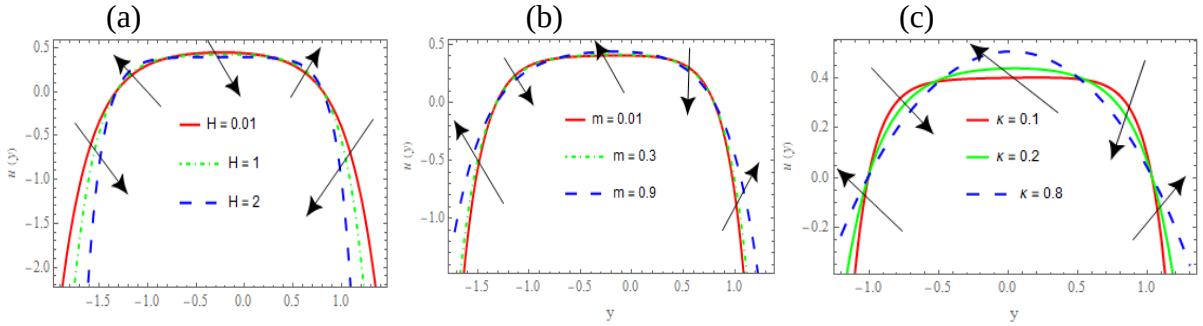

Figure 2-The velocity profile elevation via ascending value of (a) Hartman number H (b) Hall number m (c) permeability parameter κ

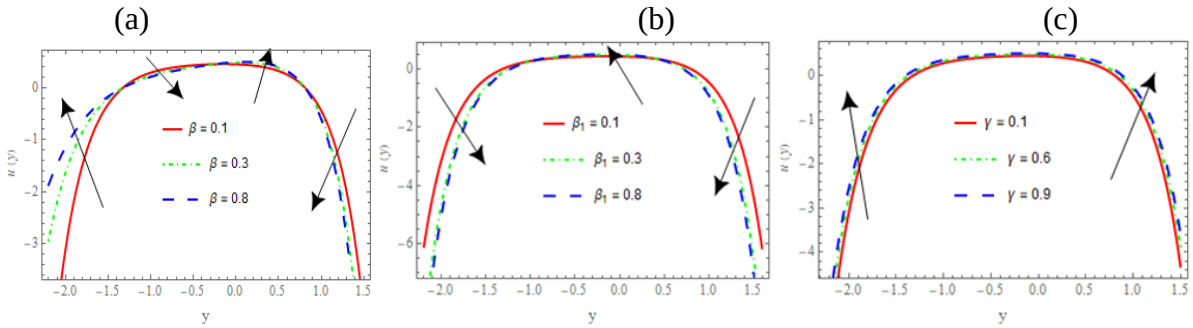

Figure 3-The velocity profile elevation via ascending value of (a) dimensionless viscosity coefficient β(b) slip parameter β_1 (c) non-uniform parameter .

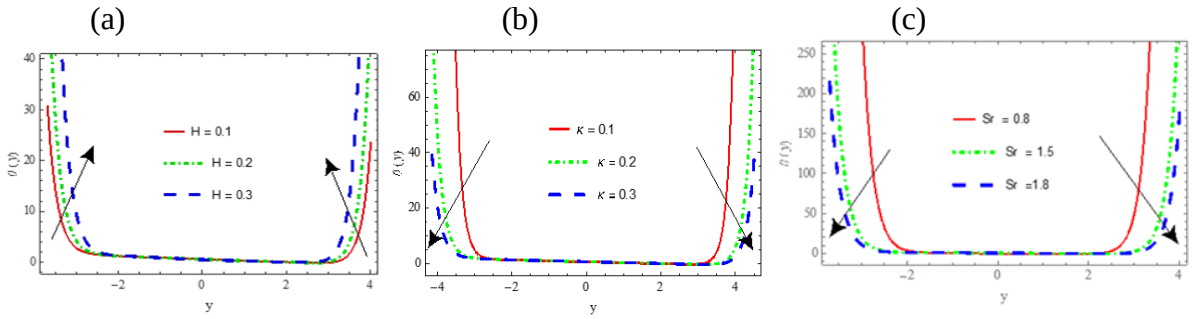

Figure 4-The temperature distribution profile elevation via ascending value of (a) Hartman number H (b) permeability parameter κ (c) Soret number Sr.

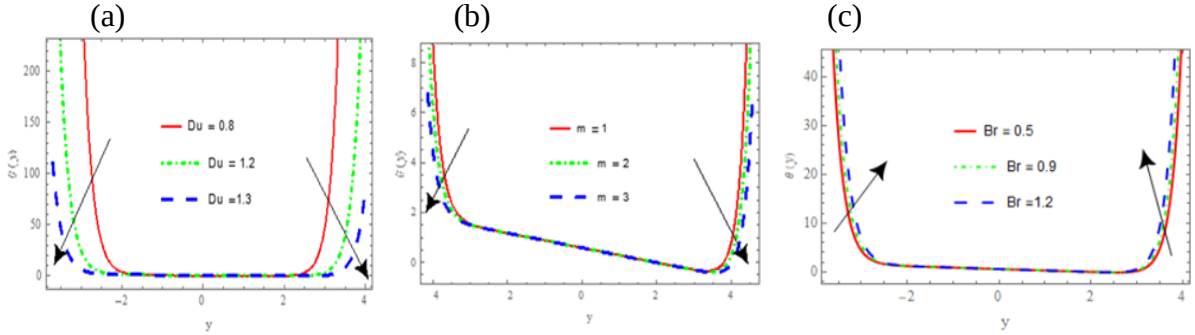

Figure 5-The temperature distribution profile elevation via ascending value of (a) Dufour number Du (b) Hall number m (c) Brinkman number Br

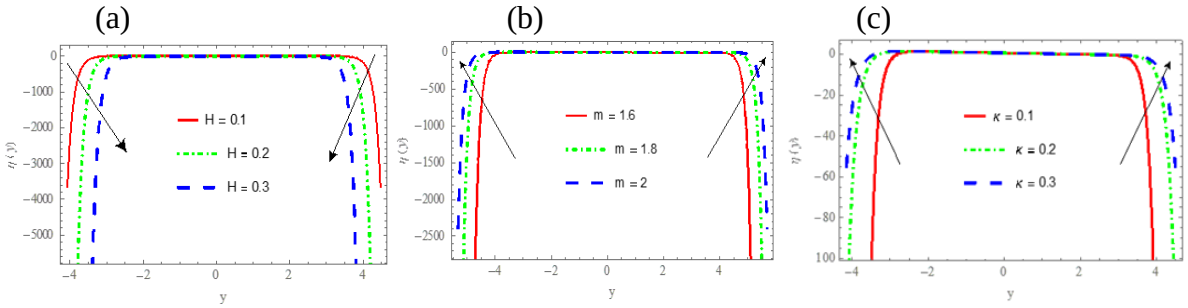

Figure 6-The fluid concentration profile variation for ascending value of (a) Hartman number H (b) Hall number m (c) permeability number κ

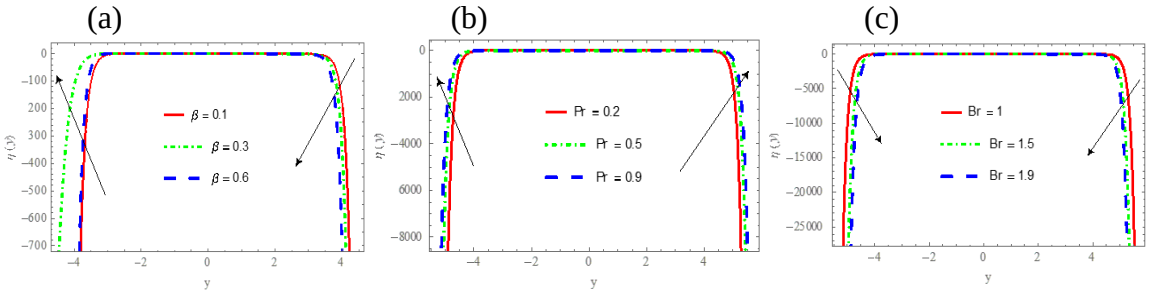

Figure 7-The fluid concentration profile variation for ascending value of (b) dimensionless viscosity parameter β (b) prandtl number Pr (c) Brinkman number Br.

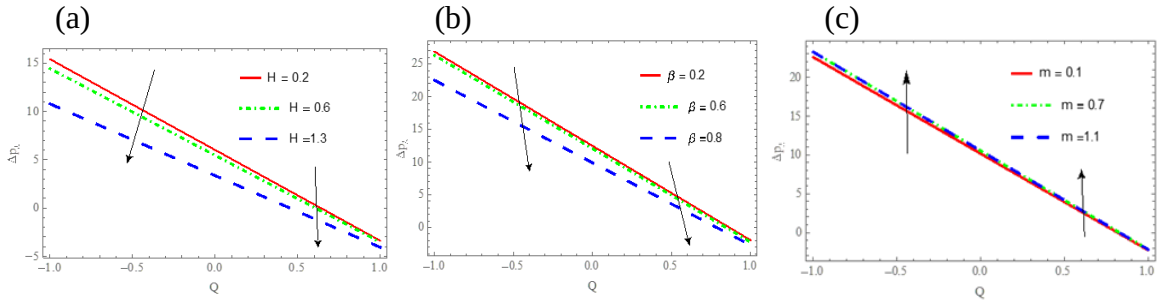

Figure 8-The pressure riseΔp_λ against elevation of (a) Hartman number H (b) dimensionless viscosity parameter β (c) Hall number m.

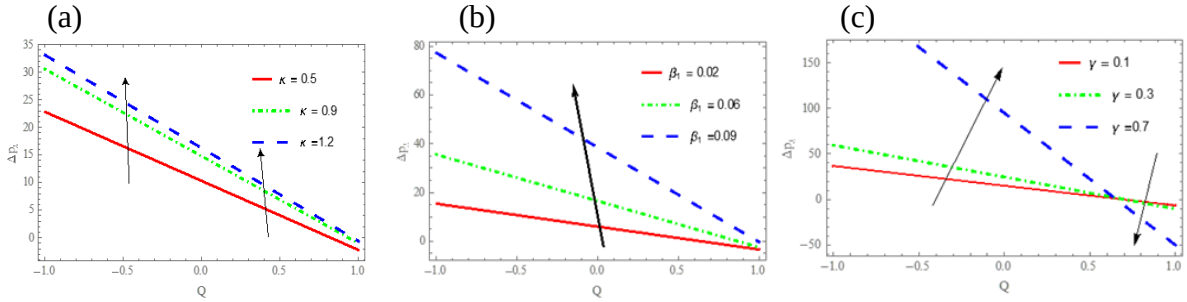

Figure 9-The pressure riseΔp_λ against elevation of (a) permeability number κ (b) slip parameter β_1(c) non-uniform parameter γ.

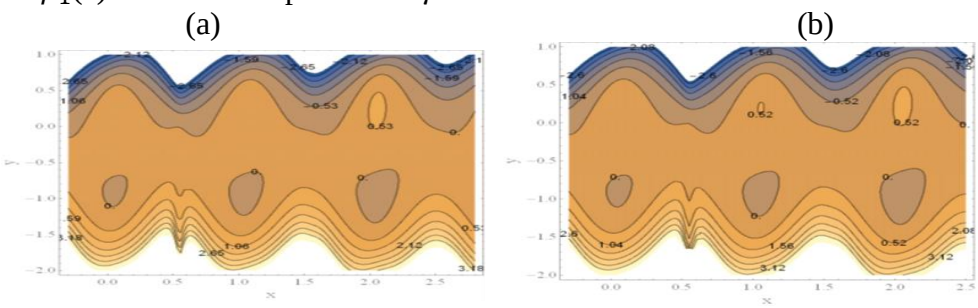

Figure- 10 The streamlines contours for elevation of Hartman number $H = \{0.1, 0.3\}$.

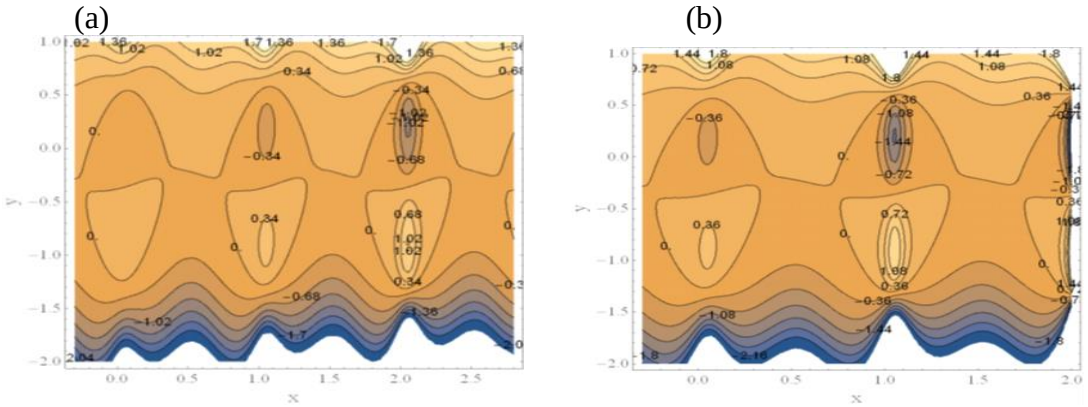

Figure-11 The streamlines contours for elevation of Hall number $m = \{0.8, 1.3\}$.

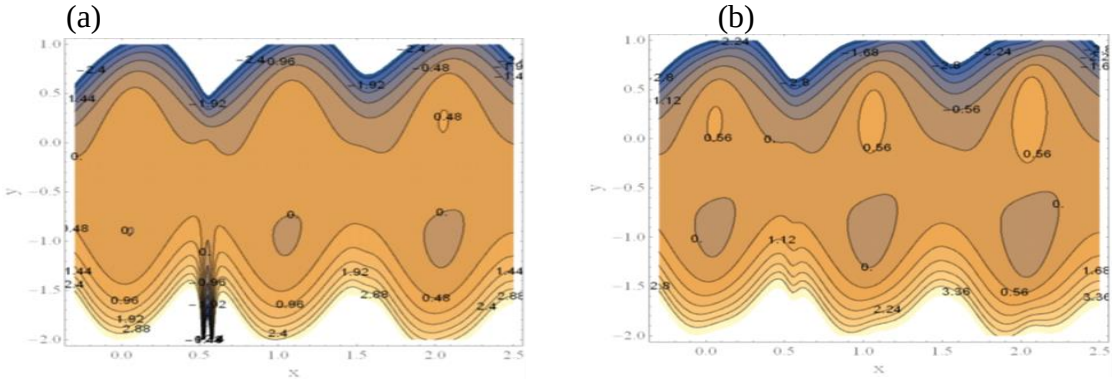

Figure 12 -The streamlines contours for elevation of permeability number $= \{0.2, 0.4\}$.

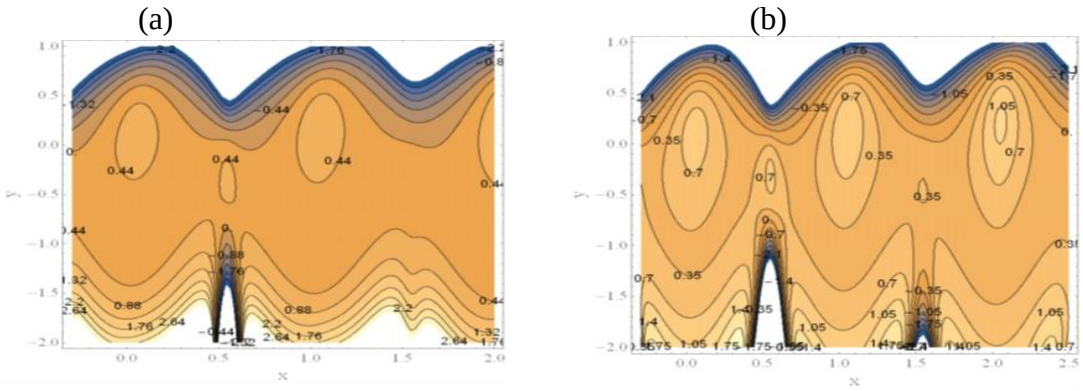

Figure 13-The streamlines contours for elevation of dimensionless viscosity parameter $= \{0.4, 0.6\}$.

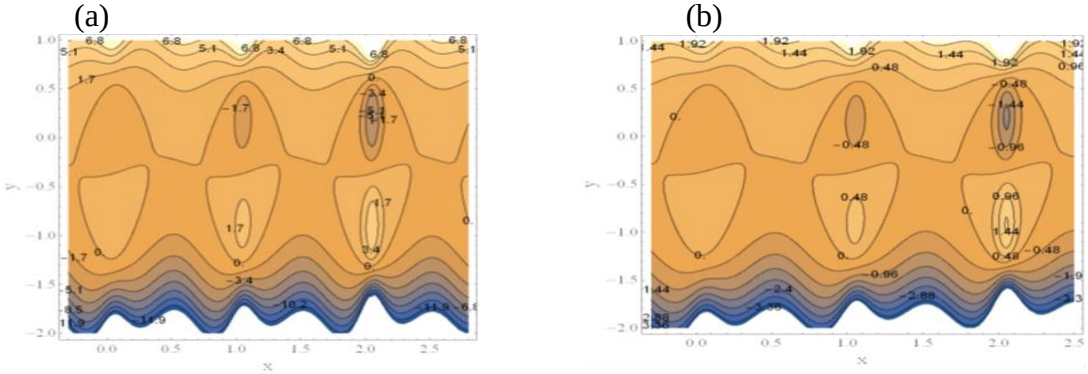

Figure 14-The streamlines contours for elevation of time flow rate parameter $Q = \{0.21, 1.1\}$.

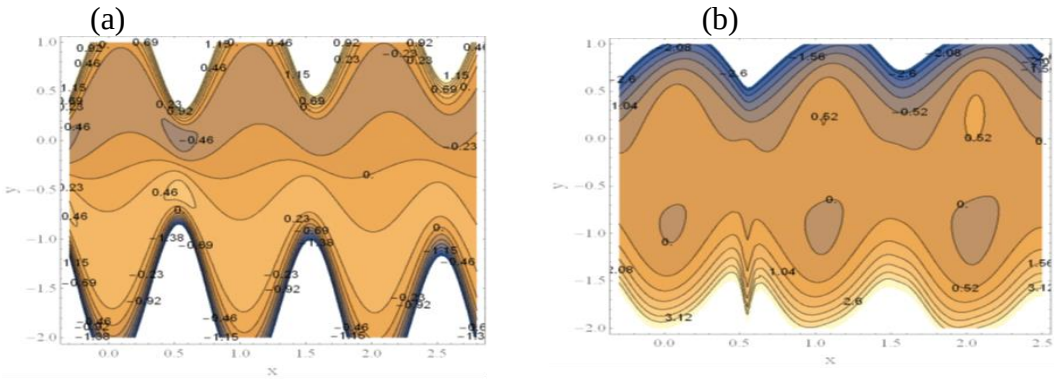

Figure 15-The streamlines contours for elevation of slip parameter $\beta_1 = \{0.1, 0.3\}$.

Conclusions

This paper devotes to inspect the effect of Hall current and varying viscosity on the peristaltic transport of viscoelastic fluid through porous medium in irregular microchannel. By considering the assumption of low Reynolds number and long wavelength, a system of nonlinear differential equations is obtained and solved for temperature field and stream function using Mathematica 11.3. The study has been come out with essential observations which are highlighted below:

The results for velocity profile of variable viscosity parameter β in this study are consistent with those in Ref. [9] for $H = m = \kappa = 0$. However, opposite result is deduced for pressure rise for β. The velocity profiles attain concave down behavior. Moreover, it is observed that the result in the center of the channel are opposite to those calculated near the boundaries. An oscillatory effect for the parameters H, m , κ, β , and β_1 on the velocity profiles is illustrated, whereas an increment impact for γ is recorded. It is evident from the plots that the temperature distribution profiles witnessed variation near the boundaries, however its value remains stable in the center of the channel. A decay in temperature distribution $\theta(y)$ is deduced via enhancement of H, Br and elevation in $\theta(y)$ is found due to the increasing of κ , Sr , Du, and m magnitudes. The patterns of concentration profile $\eta(y)$ diminishes via rise the values H, Pr, and Br, whereas, two opposite effect for β on $\eta(y)$ profile is noticed. Decreasing impact for H and β on the pressure riseΔp_λ, whilst directly effect for m, β_1 and κ on Δp_λ values. The volume and number of trapped bolus enhances for larger values of $m, \kappa, \beta_1,$ and β while, it decreased with Q, and H.

References

[1] El-Masry Y. A. S., Abd Elmaboud Y. and Abdel-Sattar M. A. **2020**. The impacts of varying magnetic field and free convection heat transfer on an Eyring–Powell fluid flow with peristalsis: VIM solution. *Journal of Taibah University for Science*, **14(**1): 19–30.

[2] Ahmed I. Abdellateef and Syed Z. Ul Haque. **2016**. Combined Effects of Hall Current and Heat Transfer on Peristaltic Transport of a Nanofluid in a Vertical Tapered Channel Through a Porous Medium. Sultan Qaboos University Journal of Science, **21**(2):107-119.

[3] Latham T.W. **1966**. Fluid motions in a peristaltic pump. M. S. thesis, Massachusetts Institute of Technology, USA.

[4] Afsar Khan A., Ellahi R. and Vafai K. **2012**. Peristaltic Transport of a Jeffrey Fluid with Variable Viscosity through a Porous Medium in an Asymmetric Channel, *Hindawi Publishing Corporation, Advances in Mathematical Physics*, **2012:** Article ID 169642, 15 pages.

[5] Noreen S., Waheed S. and A. Hussanan A. **2019**. Peristaltic motion of MHD nanofluid in an asymmetric micro-channel with Joule heating, wall flexibility and different zeta potential. *Springer Journal: Boundary Value Problems*, **12**:1-23.

[6] Awais, M., Bukhari, U., A. Ali, A. and Yasmin, H. **2017**. Convective and Peristaltic Viscous Fluid Flow with Variable Viscosity. *Journal of Engineering Thermo physics*, **26**(1): 69–78.

[7] Ali N., Hussain Q., Hayat T. and Asghar S. **2008**. Slip effects on the peristaltic transport of MHD fluid with variable viscosity. *Physics Letters A*, **372**, doi: 10.1016/j.physleta.2007.09.061.

[8] Madhia Rashid, Sohail Nadeem and Iqra Shahzadi. **2020**. Permeability impact on electromagnetohydrodynamic flow through corrugated walls of microchannel with variable viscosity. *Advances in Mechanical Engineering*, **12**(7): 1–11.

[9] Prakash J., Siva E. P., Govindarajan A. and Vidhya K. **2018**. Influence of Variable Viscosity on Peristaltic Motion of a Viscoelastic Fluid in a Tapered Microfluidic Vessel. *International Journal of Engineering & Technology*, **7**(4.10): 49-54.

[10] Nadeem S., and Noreen Sher Akbar. **2009**. Effects of heat transfer on the peristaltic transport of MHD Newtonian fluid with variable viscosity: Application of Adomian decomposition method. *Commun Nonlinear Sci Numer Simulat*, **14** (2009):3844–3855.

[11] Veera Krishna M., Bharathi K. and Chamkha A. J. **2018**. Hall Effects on MHD Peristaltic Flow of Jeffery Fluid through Porous Medium in a vertical. *Interfacial Phenomena and Heat Transfer*, **6**(3):253–268.

[12] Nabil T. M. El-dabe, Galal M. Moatimid, Mohamed A. Hassan and Wessam A. Godh. **2019**. The Hall Currents and Ion Slip Effects on a Peristaltic MHD Nanofluid with Suspended Particles. *International Journal of Applied Engineering Research*, **14(**20): 3935-3945.

[13] Asha S. K., and Deepa C. K. **2019**. Impacts of hall and heat transfer on peristaltic blood flow of a MHD Jeffrey fluid in a vertical asymmetric porous channel. *Int. J. Adv. Appl. Math. and Mech*, **6**(4):55 – 63.

[14] Mohammed R. Salman , Hayat A. Ali .**2020**. Approximate Treatment for The MHD Peristaltic Transport of Jeffrey Fluid in Inclined Tapered Asymmetric Channel with Effects of Heat Transfer and Porous Medium. *Iraqi Journal of Science*, **61**(12*): 3342-3354.*

[15] Bhatti M.M., Ali Abbas M. **2016**. Simultaneous effects of slip and MHD on peristaltic blood flow of Jeffrey fluid model through a porous medium. *Alexandria Engineering Journal*, **55**: 1017-1023.

[16] Saba S. Hasen, and Ahmed M. Abdulhadi. **2020**. MHD Effect on Peristaltic Transport for Rabinowitsch Fluid through A Porous Medium in Cilia Channel. *Iraqi Journal of Science*, **61**(6): 1461-1472.